# Journal of Visualized Experiments

## Human iPSC-Derived Cardiomyocyte Networks on Multiwell Micro-Electrode Arrays for Recurrent Action Potential Recordings
### --Manuscript Draft--

| | |
|---|---|
| Article Type: | Invited Methods Article - JoVE Produced Video |
| Manuscript Number: | JoVE59906R2 |
| Full Title: | Human iPSC-Derived Cardiomyocyte Networks on Multiwell Micro-Electrode Arrays for Recurrent Action Potential Recordings |
| Keywords: | iPSC-derived cardiomyocytes, multi-electrode array, action potential, field potential, cardiac electrophysiology, electroporation, drug screening |
| Corresponding Author: | Rosy Joshi-Mukherjee<br>Aurora Health Care<br>Milwaukee, Wisconsin UNITED STATES |
| Corresponding Author's Institution: | Aurora Health Care |
| Corresponding Author E-Mail: | rosy.joshi-mukherjee@aurora.org |
| Order of Authors: | Viviana Zlochiver |
| | Stacie L. Edwards |
| | Christopher R. Beal |
| | Jonathan A. Cook |
| | Rosy Joshi-Mukherjee |
| Additional Information: | |
| Question | Response |
| Please indicate whether this article will be Standard Access or Open Access. | Open Access (US$4,200) |
| Please indicate the **city, state/province, and country** where this article will be **filmed**. Please do not use abbreviations. | Milwaukee, WI, USA |

1    **TITLE:**
2    Human iPSC-Derived Cardiomyocyte Networks on Multiwell Micro-Electrode Arrays for
3    Recurrent Action Potential Recordings
4
5    **AUTHOR AND AFFILIATIONS:**
6    Viviana Zlochiver[1]*, Stacie L. Edwards[1]*, Christopher R. Beal[1], Jonathan A. Cook[1], Rosy Joshi-
7    Mukherjee[1, 2]
8    [1]Aurora Research Institute, Advocate Aurora Health Care, Milwaukee, WI, USA
9    [2]Department of Biomedical Engineering, College of Engineering and Applied Science, University
10   of Wisconsin-Milwaukee, WI, USA
11   *Equal contribution
12
13   **Email addresses:**
14   Viviana Zlochiver: viviana.zlochiver@aurora.org
15   Stacie L. Edwards: stacie.edwards@aurora.org
16   Christopher R. Beal: christopher.beal@aurora.org
17   Jonathan A. Cook: jonathan.cook@aurora.org
18   Rosy Joshi-Mukherjee: rosy.joshi-mukherjee@aurora.org
19
20   **Corresponding Author:**
21   Rosy Joshi-Mukherjee
22

23   **KEYWORDS:**
24   iPSC-derived cardiomyocytes, multi-electrode array, action potential, field potential, cardiac
25   electrophysiology, electroporation, drug screening
26

27   **SUMMARY:**
28   This article contains a set of protocols for the development of human induced pluripotent stem
29   cell-derived cardiomyocyte (hiPSC-CM) networks cultured on multiwell MEA plates to reversibly
30   electroporate the cell membrane for action potential measurements. High-throughput
31   recordings are obtained from the same cell sites repeatedly over days.
32

33   **ABSTRACT:**
34   Cardiac safety screening is of paramount importance for drug discovery and therapeutics.
35   Therefore, the development of novel high-throughput electrophysiological approaches for hiPSC-
36   derived cardiomyocyte (hiPSC-CM) preparations is much needed for efficient drug testing.
37   Although multielectrode arrays (MEAs) are frequently employed for field potential
38   measurements of excitable cells, a recent publication by Joshi-Mukherjee and colleagues
39   described and validated its application for recurrent action potential (AP) recordings from the
40   same hiPSC-CM preparation over days. The aim here is to provide detailed step-by-step methods
41   for seeding CMs and for measuring AP waveforms via electroporation with high precision and a
42   temporal resolution of 1 μs. This approach addresses the lack of easy-to-use methodology to gain
43   intracellular access for high-throughput AP measurements for reliable electrophysiological
44   investigations. A detailed work flow and methods for plating of hiPSC-CMs on multiwell MEA

45   plates are discussed emphasizing critical steps wherever relevant. In addition, a custom-built
46   MATLAB script for rapid data handling, extraction and analysis is reported for comprehensive
47   investigation of the waveform analysis to quantify subtle differences in morphology for various
48   AP duration parameters implicated in arrhythmia and cardiotoxicity.
49
50   **INTRODUCTION:**
51   Human induced pluripotent stem cell-derived cardiomyocytes (hiPSC-CMs) are the gold standard
52   for an increasing number of laboratories[1-10]. Beating embryoid bodies[11-13] and monolayer[3,7,10-17]
53   differentiation are the preferred methods for cardiomyocyte production and the multielectrode
54   array (MEA) has become a common modality for monitoring the electrodynamics of these
55   networks[18-20]. While parameters that can be extracted from field potentials (FPs) such as beating
56   rate, amplitude, duration and RR intervals are baseline electrophysiological responses of
57   spontaneously beating monolayers[18,21-23], the action potential (AP) components underlying these
58   extracellular FP signals are difficult to extrapolate[24]. Our recent publication on the discovery of
59   an application of MEAs for direct recurrent AP measurements provides proof of methodology for
60   exemplary intracellular AP readouts with an extensive waveform analysis at various
61   repolarization phases across multiple batches of hiPSC-derived cardiomyocyte networks[3]. In the
62   study we demonstrated that the delivery of electroporating pulses to networks of hiPSC-derived
63   cardiomyocytes enables intracellular access for AP recordings. These transient AP recordings are
64   dependent on transmembrane potential recoveries observed through the injury site[3,25,26].
65   Waveforms recorded via MEA and patch- clamp in our study showed similar AP morphologies
66   thus validating the reliability of the approach[3].
67
68   A few laboratories have reported measuring APs from various electrogenic cells using custom-
69   built MEAs[18,21,26-30], but the reliability of using MEAs for consistent and recurrent AP
70   measurements was not assessed. Currently, the gold standard patch-clamp technique is limited
71   to terminal recordings[7,31] whereas, MEA-based AP measurements are transient and therefore
72   can be conducted multiple times on the same cell. We also show that one can easily record high-
73   quality AP signals in the millivolt range requiring minimal filtering. Researchers can therefore
74   conduct not only acute but also chronic drug studies in the same preparations using MEAs.
75   Additionally, this technology permits simultaneous FP/AP measurement generating electro-
76   biome libraries in a short period of time. Given the growing emphasis on arrhythmia prediction
77   and drug associated cardiotoxicity[24,32-35], integration of AP measurement approaches will
78   enhance drug safety and efficacy assessments.
79
80   Here, we present protocols for 1) pre-plating of cryopreserved hiPSC-CMs for maturation, 2)
81   dissociating and plating of hiPSC-CMs on multiwell MEAs, 3) recording of FPs and APs from hiPSC-
82   CM networks, 4) segmenting and extracting the data for analysis, and 5) restoring the arrays for
83   multiple reuse. Each step has been optimized emphasizing critical steps wherever relevant.
84   Requirements for cell attachment to ensure a beating syncytial monolayer are discussed and
85   procedures for multiwell MEA restoration for repetitive electrophysiological studies are
86   explained. Finally, a custom GUI developed in the laboratory is presented for AP signal extraction,
87   quality assurance, and segmentation workflow to quantify and analyze AP parameters.
88

**PROTOCOL:**

**1.     Preparation of solutions and materials (see Table of Materials)**

**1.1.     6-well tissue-culture plate substrate-coating**

1.1.1.   Thaw the coating substrate on ice or at 4 °C.

1.1.2.   Prepare a 1:100 coating substrate dilution in cold DMEM/F12 medium. Mix the solution by slow pipetting.

1.1.3.   Transfer 2 mL of the coating substrate solution (step 1.1.2) per well of a 6-well tissue culture plate.

1.1.4.   Immediately place the coated tissue culture plate in the cell culture incubator at 37 °C and 5% $CO_2$ for at least 7 h and use within 7 days.

**1.2.     hiPSC-CM culture medium**

1.2.1.   Add 10 mL of CM media supplement thawed at 4 °C to 500 mL of CM base medium. Store at 4 °C for up to 2 weeks.

1.2.2.   Aliquot required amount of media for the day and bring to room temperature before use.

1.3.     hiPSC-CM thawing medium: Prepare fresh by mixing hiPSC-CM culture medium (step 1.2) with 10% fetal bovine serum (FBS). Bring the media to room temperature prior to thawing of CMs for suspension.

1.4.     Fibronectin 1 mg/mL stock solution: Aliquot 200 μL into 1.5 mL sterile microfuge tubes and stored at 4 °C for later use. Prepare working solution of 50 μg/mL concentration freshly on ice.

1.5.     Multiwell cleaning solution: Combine 0.5 g of enzymatic detergent with 50 mL of sterile double distilled water (ddH₂O). Vortex to mix the contents. Filter and store at 4 °C for up to a week.

**2.     Pre-plating of cryopreserved hiPSC-CM for maturation (Figure 1)**

NOTE: This section is intended for thawing and culturing hiPSC-CMs that were differentiated using the feeder-free monolayer method[3,16] and cryopreserved in liquid nitrogen 10 days post-differentiation at 1-2 million cells/vial. Cells from one vial are plated into two substrate-coated wells of a 6-well tissue culture plate. Cardiomyocytes tend to settle at the bottom of the tube so gentle mixing at the time of pre-plating is important for achieving even cell density across wells.

133 2.1. Aliquot 2 mL of FBS per vial of hiPSC-CMs being thawed into a 15 mL conical tube and
134 bring to room temperature.

136 2.2. Thaw vials of cryopreserved hiPSC-CMs by placing them in a 37 °C water bath and swirl
137 gently for even thawing for no more than 3 min.

139 2.3. Immediately transfer the vial contents to the tube containing FBS (see step 2.1), mix by
140 swirling and centrifuge at 200 x $g$ for 5 min.

142 2.4. Aspirate the supernatant and resuspend the cell pellet in 1 mL of hiPSC-CM thawing
143 medium (see step 1.3) per vial thawed. Use a transfer pipette to resuspend the pellet by gentle
144 trituration. Assess cell viability.

146 2.5. Add additional 3 mL of thawing medium per vial of hiPSC-CM thawed in step 2.4 and
147 suspend gently using a transfer pipette to further dissociate cell clumps.

149 2.6. Dispense 2 mL of cell suspension gently into each well of substrate-coated 6-well plates
150 (see step 1.1). Place in cell culture incubator at 37 °C and 5% $CO_2$.

152 2.7. Replace with fresh hiPSC-CM culturing medium after 24 h and 3 times weekly thereafter
153 for 20 days.

155 NOTE: Cells should adhere to the substrate coating by 24 h and beat spontaneously at 48 h post-
156 plating (See **Video 1** and **Video 2**).

158 **3. Multiwell MEA plate sterilization and coating (Figure 2 and Figure 3)**

160 NOTE: The protocol described here is for preparing 24-well MEA plates with 12 micro gold PEDOT-
161 coated electrodes on glass for hiPSC-CM plating. Avoid touching the bottom of the plate as this
162 may damage the electrodes.

164 3.1. Two days prior to cell plating, add 0.5 mL of hiPSC-CM culture medium (see step 1.2) to
165 each well and perform a baseline recording to verify signal-to-noise ratio for quality check of the
166 MEAs.

168 3.2. Aspirate the media, rinse with sterile $ddH_2O$ and sterilize under UV light inside a laminar
169 flow hood overnight.

171 3.3. The day prior to cell plating, add 0.1 mL of FBS to each well for hydrophilic treatment of
172 MEA surfaces. Incubate for 30 min at room temperature. This step is necessary for cell
173 attachment.

175 3.4. Aspirate the FBS and rinse with 0.5 mL of sterile $ddH_2O$ per well. Repeat one more time.
176

177 <mark>3.5.    Leave the plate to dry in the laminar flow hood overnight.</mark>

178

179 3.6.    Prepare a working dilution of 50 µg/mL fibronectin in cold DMEM/F12 medium from the
180 stock (see step 1.4). Keep the solution on ice.

181

182 3.7.    <mark>Pipette 5 µL of the working fibronectin dilution (see 3.6) and carefully dispense the</mark>
183 <mark>droplet to the center of each well to cover all 12 electrodes.</mark> It is important to work swiftly across
184 the 24 wells to prevent the droplet from drying.

185

186 3.8.    <mark>Immediately place the fibronectin-coated multiwell MEA plate on a raised surface inside</mark>
187 <mark>a humidifying chamber containing sterile ddH$_2$O to cover the entire dish surface. Place the</mark>
188 <mark>chamber with the multiwell MEA plate for 3 h in the cell culture incubator.</mark>

189

190 3.9.    <mark>When ready for plating, carefully remove the fibronectin drop using a P10 pipette and</mark>
191 <mark>plate hiPSC-CMs immediately. It is critical to perform this step one well at a time to prevent</mark>
192 <mark>fibronectin from drying.</mark>

193

194 NOTE: Placing the 24 well MEA plate in a humidifying chamber is critical to prevent fibronectin
195 droplets from drying out during the incubation period.

196

197 <mark>**4.    hiPSC-CM dissociation and plating on Multiwell MEA plate (Figure 3)**</mark>

198

199 NOTE: Start this step about 1 h prior to MEA fibronectin incubation is complete. Ensure that the
200 cell dissociation solution is at 37 °C and the iPSC-CM thawing medium is at room temperature.
201 Dissociation methods have been optimized for 30 days post-differentiated hiPSC-CMs cultured
202 on substrate-coated 6-well plates (see step 2) to obtain about 90% viable CMs for MEA plating.
203 Care should be taken not to introduce air bubbles while trituration to prevent cell death.

204

205 4.1.    Aspirate the culture medium from each well of the 6-well tissue culture dish with 30 day
206 post-differentiated hiPSC-CM culture (see step 2.7) and wash with 2 mL of sterile D-PBS per well.

207

208 4.2.    Add 1 mL of pre-warmed cell dissociation solution (see **Table of Materials**) per well and
209 incubate for 4 min at 37 °C. Use a transfer pipette to gently triturate to loosen cells for
210 dissociation. If most of the cells are still adherent, incubate for another 3 min at 37 °C and
211 triturate again. This additional incubation should help for maximal cell recovery. Do not incubate
212 for more than 7 min as this might result in low cell viability.

213

214 4.3.    Using a transfer pipette, pool all the dissociated cells into a conical tube containing hiPSC-
215 CM thawing medium (see step 1.3). It is recommended to suspend the cells in at least twice the
216 volume of media (2 mL per well being harvested) to block the activity of the cell dissociation
217 solution.

218

219 4.4.    Centrifuge at 200 x *g* for 5 min.

220

221  4.5.     Aspirate the solution carefully as the pellet is loosely attached to the surface and
222  resuspend in 0.1 mL of hiPSC-CM thawing medium. Use a transfer pipette to resuspend the pellet
223  a few times by gentle trituration.
224
225  4.6.     Aliquot 2 µL of dissociated cells and dilute with 18 µL of media in a 1.5 mL microfuge tube.
226  Add 20 µL of Trypan Blue and mix for cell count and viability assessment.
227
228  4.7.     Adjust the cell density to 6,000 cells/µL by adding the appropriate volume of hiPSC-CM
229  thawing medium. Suspend the pellet by gentle flicking a few times. The hiPSC-CMs easily detach
230  from glass surfaces especially when plated at high densities. We have optimized the seeding
231  density and plating conditions to achieve 15 days of electrical recordings.
232
233  4.8.     When ready, bring the multiwell MEA plate into the laminar flow hood for cell seeding. It
234  is critical to perform the following two steps one well at a time to prevent the fibronectin from
235  drying.
236
237  4.8.1.   Carefully remove the fibronectin droplet using a P10 pipette without touching the
238  electrodes.
239
240  4.8.2.   Immediately dispense a 5 µL cell droplet (30,000 cells) to the center of the well of the
241  MEA plate covering all 12 electrodes. Repeat the step until all the 24 wells are plated.
242  Intermittent mixing of cell suspension by flicking is recommended.
243
244  4.9.     Place the multiwell MEA plate back in the loosely covered humidifying chamber and
245  return to the cell culture incubator at 37 °C and 5% $CO_2$ for 3 h for cell attachment.
246
247  4.10.    Carefully add 200 µL of hiPSC-CM thawing medium to each well without disturbing the
248  cell droplets using a P200 pipette. Add the media dropwise to the side of the well.
249
250  4.11.    Place the multiwell MEA plate back in the cell culture incubator.
251
252  4.12.    Replace with fresh hiPSC-CM culture medium at 24 h post plating. Spontaneous beating
253  of cardiomyocytes can be observed at this point (See **Video 3**).
254
255  4.13.    Change the media every 2 days until the end of experiments.
256
257  **5.     hiPSC-CM electroporation and signal acquisition (Figures 4 – 6)**
258
259  NOTE: This protocol is for simultaneous recording of high-throughput electrode signals (12 sites
260  for each of the 24 wells). The 24-well multiwell MEA system is used with the acquisition software
261  (see **Table of Materials**). All MEA recordings are conducted at 37 °C.
262
263  5.1.     Turn on the interface board and initiate the acquisition software. Allow enough time for
264  the multiwell MEA headstage to reach 37 °C temperature (see arrow no. 1 in **Figure 4**).

265

266 5.2.    Insert multiwell MEA plate from step 4 into the multiwell MEA headstage by placing it
267 covered over the recording platform and click the **Insert** button (see arrow no. 2 in **Figure 4**).
268 Allow for temperature to stabilize before starting recordings.

269

270 5.3.    **Adjust acquisition and electroporation settings**

271

272 5.3.1.  Click on the **Define Experimental Flow** icon (see arrow no. 3 in **Figure 4**) and set recording
273 time to 2 min or as desired.

274

275 5.3.2.  Click on the **Data Acquisition Setup** icon (see arrow no. 4 in **Figure 4**) and set sampling
276 rate to 20 kHz, high-pass filter to 0.1 Hz and low-pass filter to 3500 Hz.

277

278 5.3.3.  Click on the **Stimulator Settings** icon (see **Figure 5**). Under the **Stimulus Definition** tab,
279 define stimulation as biphasic symmetric voltage pulses of 1 mV, 1 ms and 1 Hz. Under the
280 **Stimulation Electrodes** tab, select electroporation sites by highlighting all relevant electrodes.

281

282 5.4.    Click the **Explore** button to visualize signals in all wells. Verify signal quality and steady
283 state conditions. Take notes on electrodes with FP signals in the mV range. Click the same button
284 to stop the exploration. No data has been recorded up to this point.

285

286 5.5.    Start recording by clicking on the **Go!** button. The electrodes in each well will show FP
287 signals in the raw data window (**Figure 6**). After 30 s of recording, click on the **Stimulate** button
288 and allow electroporation to take place on the selected sites for 30 s; then, click on the same
289 button to stop stimulation and continue recording for the remaining 60 s.

290

291 NOTE: The recorded file can be played back by switching to 'Replayer Mode' in the 'Application'
292 dropdown menu.

293

294 **6.    Multiwell MEA plate cleaning for reuse**

295

296 6.1.    After final experiments, clean all the wells in the multiwell plate by aspirating all media
297 contents from each well and carefully avoiding touching the electrode surface.

298

299 6.2.    Add 1 mL of sterile ddH$_2$O per well. Aspirate and repeat once.

300

301 6.3.    Add 0.3 mL of multiwell cleaning solution (see step 1.5) per well. Incubate overnight at
302 room temperature to dislodge cells and debris.

303

304 6.4.    The following morning, aspirate the solution and rinse with 1 mL of sterile ddH$_2$O.
305 Incubate for 5 - 7 min and aspirate. Repeat 5 times.

306

307 6.5.    Add 0.5 mL of sterile ddH$_2$O per well. Record the baseline of the cleaned multiwell plate
308 for quality check of the cleaned MEAs (**Figure 7**).

309

310   6.6.    Store at 4 °C until ready to use.

311

312   **7.    Data file conversion and export**

313

314   NOTE: Four data files will be generated for every recording: MWR, MWC, MWD, and MWS files.
315   Using the converter software, the MWD file can be converted to H5 file for subsequent analysis
316   using custom-built script (see **Supplementary File 1**).

317

318   7.1.    Initiate the converter software (see **Table of Materials**).

319

320   7.2.    Select **Set Input Path** from the **File** menu. Select folder containing data files of interest.

321

322   7.3.    Select **Set Output Path** from the **File** menu. Select folder where converted files are to be
323   saved.

324

325   7.4.    Highlight MWD file of interest.

326

327   7.5.    Click the **EXPORT to HDF5** button.

328

329   **8.    Data segmentation and analysis (Figures 8-10)**

330

331   NOTE: Matlab-based custom software is used to segment and extract various FP and AP data
332   parameters. Software is available on demand.

333

334   8.1.    Run the **Waveform Analysis** code using Matlab (see **Figure 8** for a view of the GUI's main
335   window).

336

337   8.2.    Click on **File** and select **Process .h5**.

338

339   8.3.    Find and select the mwd.h5 file created according to step 7 above.

340

341   8.4.    Click on the **Save Directory** button to change the storage location of the output files.

342

343   8.5.    Create a signal processing queue by selecting electrode/well combinations of interest and
344   then clicking on the **Queue** button. Repeat this step to append more electrode/well combinations
345   to be processed to the queue.

346

347   8.6.    Edit the queue by clicking directly on **Med Name / Med Concentration** if cells were
348   treated with drugs (**Figure 8**).

349

350   8.7.    Once the queue is final, click the **Initialize Waveforms** button. This will start the
351   preliminary processing in which signals are identified and extracted for segmentation.

352

8.8.     Click on the **Zoom In** button and select the action potential area of interest with the cursor
354   (**Figure 9**).

356   8.9.     Click the **Keep** button and review the panels. Peaks (red 'x') and troughs (yellow circles)
357   are detected for every waveform and the normalized action potentials are superimposed. Click
358   the **Keep** button and move on to the next trace in the queue (**Figure 10**).

360   8.10.    Repeat steps 8.8-8.9 for the rest of the electrode/well combination signals in the queue.

362   NOTE: A **.csv** file will be generated with APD parameters measured for every waveform. A **.mat**
363   file for each **.h5** file is also saved to allow additional processing of segmented data.

365   **REPRESENTATIVE RESULTS:**
366   The viability and plating density of post-thawed hiPSC-CMs is critical for multiwell MEA culture.
367   Pre-plating of 1-2 million hiPSC-CMs/vial into two wells of a 6-well tissue culture plate with 50%
368   or greater viability will produce a healthy monolayer culture with spontaneous beating at 48 h.
369   Poor viability of CMs will result in cultures with a high percentage of non-myocyte populations.
370   These monolayers when dissociated for multiwell MEA plating generally produce inconsistent
371   results and bad quality signals and therefore should be discarded. **Figure 1** shows examples of
372   optimal vs. sub-optimal hiPSC-CMs cultures at 48 h post plating. Thawing the CMs on substrate-
373   coated tissue culture plates rather than directly on multiwell MEAs, allows for cell recovery and
374   maturation[3]. Direct plating of cryopreserved CMs on the array is not recommended as it
375   produced inconsistent results.

377   In addition to the quality of the dissociated CMs, cell attachment on multiwell MEA is highly
378   dependent on cell density and the fibronectin coating technique. The fibronectin droplet size is
379   critical as the CMs will conform to the boundaries of the fibronectin-coated area. For this reason,
380   only 5 µL of the fibronectin solution are dispensed directly over the electrode array area. To
381   ensure that the droplet does not disperse, the well surface must be completely dry at the time
382   of coating. **Figure 2** shows the layout of the multiwell MEA plate with schematics of step-by-step
383   pretreatment for optimal preparation. Additionally, to prevent the fibronectin from drying the
384   multiwell MEA plates must be placed inside a humidifying chamber during the incubation period
385   lasting no more than 3 h (see step 3.8). Once the incubation period is complete, it is important
386   to remove the fibronectin droplet from each well just before CM plating and only then proceed
387   to next well plating. Working swiftly and carefully dispensing of the CMs is the key to successful
388   cell attachment.

390   hiPSC-CM cultures at 30 days post-differentiation are dissociated for multiwell MEA plating using
391   the enzymatic cell dissociation method (see step 4). CMs will attach to the fibronectin-coated
392   MEA surfaces by 3 h and a monolayer covering the arrays will be visible after 24 h post-plating
393   (**Figure 3**). Synchronous beating of the monolayer will be observed at 24-48 h. Cell droplet
394   dispersion will affect the culture density or even lead to drying and cell death. Precise cell
395   placement directly on the array is of utmost importance and therefore the technique must be
396   practiced for optimal plating. Cell adhesion to the reference electrode will hinder electrical signal

397     production. See **Figure 3** for images of optimal CM placement, and culture after 24 h.
398
399     The CMs cultured on multiwell MEAs are subjected to quality check for electrical activity at 48 h
400     post-plating. Typically, FP signal amplitude increases from the μV range to mV in approximately
401     4 days[3]. If 50% of the electrodes within a network and 70% of the total networks do not produce
402     FP signals, then the network or the culture are suboptimal and should be discarded. Only cultures
403     that pass the quality check are processed for FP and AP analysis. **Figure 6** shows examples of
404     good and sub-standard FP signals.
405
406     Electroporation-mediated AP recordings can be obtained multiple times from cultures 48 h post-
407     MEA plating. Employing electroporation, we gained intracellular access to record high-resolution
408     APs from multiple hiPSC-derived cardiomyocyte networks. Low-voltage pulses (1 V, 1 ms, 1 Hz)
409     for 30 s were delivered for transient, reversible transformation of FP to AP. The electroporation
410     allows successful intracellular access for AP measurement in approximately 75% of the
411     electrodes. Electrical signals are recorded for 2 min that include 30 s pre-electroporation, 30 s
412     during and 1 min post-electroporation. A train of 10 s AP waveforms 10 s post-electroporation
413     are evaluated across all sites for signal quality and analysis. Any trace not conforming to pure AP
414     signal are discarded. To investigate if AP amplitudes correlate to FP signal we electroporated all
415     288 sites to simultaneously record waveforms. Representative FP and AP signals recorded from
416     the same cell site from two different electrodes are shown in **Figure 11A**. We observed no
417     correlation between FP amplitudes and post electroporation AP amplitudes recorded from the
418     same cell site. Additionally, multiple electroporations of the same cell site at 0, 24, 48, 72 and 96
419     h had no significant effect on the AP shape over time (**Figure 11B**).
420
421     Given the high-throughput nature of the system, a manual technique to extract and quantify
422     parameters of interest such as RR interval, instantaneous frequency and differential action
423     potential duration is inefficient and time consuming. A custom-built MATLAB script available to
424     the research community upon request is employed to perform waveform measurements with 1
425     μs resolution. Electroporation time points are overlaid with the extracted signal to identify 10 s
426     of AP post-electroporation to conduct signal extraction, quality assurance, and segmentation
427     workflow (**Figures 8-10**). The user interface allows for selection of the desired segment using the
428     overlaid electroporation indicators as a guide. The segmented waveform is processed by
429     subroutines to further identify individual AP waveforms. This is completed through peak
430     detection, where the highest and lowest voltage is identified for each cycle. Once this process is
431     completed, the amplitudes are normalized, and the associating time vectors are shifted to define
432     time zero at a peak value of 1. Interpolation of intersection points along the individual cycles was
433     used to determine APD measurements. Thus, partial automation workflow for AP waveform
434     segmentation allows efficient data analysis for various APD parameters across multiple batches
435     of cultures in a short period of time. Further automation of inclusion and exclusion criteria for
436     FPs and APs is ongoing for real-time data analysis.
437
438     A significant advantage of the multiwell MEA plate is that it can be reused multiple times. This
439     restoration enables repetitive electrophysiological studies for cost-effective and consistent data
440     collection. Recordings of APs from the same array after 6 restorations are shown in **Figure 12**.

441 Signal-to-noise ratio is similar across multiple reuses. To demonstrate the reliability of the array
442 for repetitive electrophysiological studies, a total of 3815 AP waveforms are pooled from three
443 restoration batches and AP duration data is extracted to examine the repeatability of the results.
444 Distribution plots for individual waveform $APD_{30}$, $APD_{80}$, triangulation ($APD_{80}$—$APD_{30}$) and
445 fractional shortening (($APD_{80}$—$APD_{30}$)/($APD_{80}$)) are displayed (**Figure 13**).
446
447 **FIGURE LEGENDS:**
448 **Figure 1: Pre-plating of cryopreserved hiPSC-CM for maturation.** (**A**) Cell processing for pre-
449 plating 1 vial of 10 days post-differentiation cryopreserved hiPSC-CMs. (**B**) Phase contrast images
450 of successful (left) and unsuccessful (right) hiPSC cultures. Scale bar: 275 µm. See **Video 1** and
451 **Video 2** for successful 14 and 24 days post-differentiation culture examples.
452
453 **Figure 2: Multiwell MEA plate setup and preparation.** (**A**) Multiwell MEA plate schematics: The
454 plate consists of 24 wells (A1 through D6) each containing 12 microelectrode arrays and 4
455 peripheral reference electrodes. Electrode diameter: 30 µm / Inter-electrode distance: 300 µm.
456 Recordings can be obtained from the 288 electrodes simultaneously. (**B**) Sterilization and
457 hydrophilic treatment steps to be conducted prior to hiPSC-CM plating.
458
459 **Figure 3: hiPSC-CM dissociation and plating on Multiwell MEA plate.** (**A**) Schematics of hiPSC-
460 CM MEA plating steps for each well. (**B**) Microscopic image illustrating correct cell droplet
461 placement covering all 12 electrodes without spreading to the 4 reference electrodes. (**C**) Phase
462 contrast microscopic images of an exemplary (left) and suboptimal (right) hiPSC-CM platting on
463 MEA at 24 h post-plating. Scale bar= 275 µm. See **Video 3** for successful MEA plating example.
464
465 **Figure 4: Multiwell-screen acquisition software.** Arrows indicate the location of key features and
466 functions referenced in the text: Temperature Control (1) panel allows for real time temperature
467 monitoring throughout the experiment. Insert/Eject (2) button engage and release the Multiwell
468 MEA Plate. Define Experimental Flow (3) function allows the user to set the duration of the
469 recording. Data Acquisition Setup (4) function allows the user to set the sampling rate and
470 acquisition filter settings.
471
472 **Figure 5: hiPSC-CM electroporation and signal acquisition. Stimulus Definition** tab allows the
473 user to define the electroporating pulse parameters. **Stimulation Electrodes** tab allows the user
474 to select the electroporating electrodes. Any combination of the 288 electrodes can be selected.
475
476 **Figure 6: Quality check of Multiwell MEAs for electrical activity. Multiwell**-**Screen** acquisition
477 software showing raw data windows with representative examples of optimal (**A**) and sub-
478 standard (**B**) FP signals.
479
480 **Figure 7: FP and AP signals from the new and restored array.** Multiwell MEA enzymatic cleaning
481 steps (**A**). The baseline signal of the new array shows minimal signal to noise ratio (**B**) and FP
482 signals show the electrical activity of the network (**C**).
483
484 **Figure 8: Data segmentation and analysis.** View of GUI's main window for **Waveform Analysis**.

485

486 **Figure 9: Data segmentation and analysis. Initialize Waveforms** button to identify and extract
487 AP waveforms for segmentation and to start the preliminary processing by zooming in and
488 selecting the action potential area of interest. Red circles are the electroporation indicators.

489

490 **Figure 10: Data segmentation and analysis.** Peaks (red 'x') and troughs (yellow circles) are
491 detected for every waveform and the normalized APs are superimposed for a quality check of
492 the waveforms.

493

494 **Figure 11: AP Amplitude dependence on the FP signal for multiple recordings from the same**
495 **cell site.** FP amplitude in μV ranges (**A**, top left panel) or mV ranges (**A**, top right panel) recorded
496 from two independent electrodes produce AP amplitude in mV range (**A**, bottom left and right
497 panels) showing no correlation between FP amplitudes and post-electroporation AP amplitudes.
498 The normalized AP waveforms for each recording are superimposed as shown for each recording.
499 Multiple electroporations of the same cell site at 0 to 96 h produced high quality AP waveforms
500 allowing tracking of membrane electrodynamics (**B**).

501

502 **Figure 12: AP recordings after six restorations.** AP waveforms recorded simultaneously 10 s post-
503 electroporation across 12 electrodes from the same well are displayed.

504

505 **Figure 13: APD parameter histograms from multiple restorations.** Distribution plots for
506 individual waveform $APD_{30}$ (**A**), $APD_{80}$ (**B**), triangulation ($APD_{80}$—$APD_{30}$) (**C**) and fractional
507 shortening (($APD_{80}$—$APD_{30}$)/($APD_{80}$)) (**D**) are displayed.

508

509 **Supplementary files. Videos 1-3.**

510

511 **DISCUSSION:**
512 Over the years, the application of MEAs has been limited to carrying out FP measurements of
513 excitable cells to study their electrophysiological properties[36-39]. Only a few groups have reported
514 AP traces from electrogenic cells using custom MEA based technology[18,29,30]. However, these
515 approaches have not been investigated for repeated recordings from the same preparations. We
516 developed an innovative and accurate methodology for studying APs from the same cell site over
517 days in multiple hiPSC-CM networks simultaneously[3]. In our published study, a multiwell micro-
518 gold MEA platform was employed to generate AP waveform libraries from multiple batches of
519 hiPSC-CM cultures with high precision and with a temporal resolution of 1 μs. The protocol
520 described here explains seeding of hiPSC-CMs on the array for efficient development of syncytial
521 CM networks for high-throughput AP recordings. Several critical steps in the protocol are: 1)
522 production of multiple high-purity batches of quality-controlled CMs for cryopreservation
523 banking, 2) highly viable post-thaw CMs for pre-plating and maturation, 3) treatment of the
524 multiwell MEA plate for CM seeding, 4) hiPSC-CM culture dissociation at 30 days post-
525 differentiation for MEA plating, and 5) restoration of the MEAs for multiple reuse.

526

527 It is important to note that batch-to-batch variation in hiPSC differentiation might affect
528 experimental outcomes. The monolayer method of differentiation was optimized in-house for

529  high percent cardiomyocyte production[3,40]. The FACS analysis of MLC2v and TNNT2 markers of
530  our cultures demonstrate a ≥90% ventricular-like phenotype[3]. These quality-controlled cultures
531  are cryopreserved for experimental studies. The current differentiation approaches yield a
532  heterogeneous mix of nodal-, atrial- and ventricle-like cells[3,16,17,41]. Therefore, strategies
533  employed for CM subtype population enrichment can further improve the specificity of the
534  cultures. Additionally, tissue engineering approaches can be employed to enhance their
535  maturation. The methods proposed here can easily be implemented for other CM sources.
536
537  The AP waveforms recorded using MEA were similar to those recorded from networks of
538  cardiomyocytes by optical mapping[42,43], complementary metal oxide semiconductor-based
539  MEA[18,21], and simulated AP using FP recordings[20]. To address the mechanism of AP
540  measurements via MEA Hai and Spira[25] demonstrated that electropore-electrode interface mimic
541  the established sharp glass microelectrode technique. However, the resting membrane potential
542  and true amplitude values in our study cannot be established given that the electropore-
543  electrode interface in MEA systems is not calibrated, and that the amplitude is a function of the
544  sensitivity and resolution of the technique. Our approach shares similar limitations to optical
545  mapping when it comes to AP amplitude.
546
547  The multiwell MEA-based FP/AP readouts reported here open new possibilities for drug safety
548  assessment. Although spontaneous, these hiPSC-CM monolayers beat at constant rates. Analysis
549  of APD parameters across multiple networks provide insight on electrical heterogeneity (**Figure
550  13**). However, comprehensive APD restitution analyses must incorporate preceding diastolic
551  intervals. Furthermore, high-quality AP waveforms recorded from the same cell site over 96 h
552  (**Figure 11B**) is the first report to track membrane electrodynamics over time which will be of
553  value in development and in disease.
554
555  The protocol described here for quantifying AP parameters can be used to generate dose-
556  response curves to test compounds. As recently reported by Edwards et al.[3], dose response of
557  norepinephrine, isoproterenol and E 4031 are plotted for APD at various repolarization phases.
558  The published study demonstrated the accuracy and reliability of the approach for identification
559  of the dose-dependent subtle changes in the AP waveforms in real time. This technique could
560  easily be extended for other compounds or small molecule libraries for understanding various
561  electrophysiological responses.
562
563  The MEA based approach for AP measurements presented in this study will be of interest not
564  only to electrophysiologists but also to cell biologists and *in-silico* modelers. Furthermore, FP/AP
565  recordings from the same cell site on hiPSC-CMs will enable researchers to generate bioelectric
566  data libraries of wide array of excitable cellular networks within a short period of time.
567  Availability of these resources will be valuable for drug discoveries and disease modeling.
568
569  **DISCLOSURES:**
570  The authors have nothing to disclose.
571
572  **REFERENCES:**

573   1   Dambrot, C., Passier, R., Atsma, D. & Mummery, C. L. Cardiomyocyte differentiation of
574       pluripotent stem cells and their use as cardiac disease models. *Biochemical Journal.* **434**
575       (1), 25-35, (2011).
576   2   Dunn, K. K. & Palecek, S. P. Engineering Scalable Manufacturing of High-Quality Stem Cell-
577       Derived Cardiomyocytes for Cardiac Tissue Repair. *Frontiers in medicine.* **5** 110, (2018).
578   3   Edwards, S. L. *et al.* A Multiwell Cardiac muGMEA Platform for Action Potential Recordings
579       from Human iPSC-Derived Cardiomyocyte Constructs. *Stem Cell Reports.* **11** (2), 522-536,
580       (2018).
581   4   Herron, T. J., Lee, P. & Jalife, J. Optical imaging of voltage and calcium in cardiac cells &
582       tissues. *Circulation Research.* **110** (4), 609-623, (2012).
583   5   Huebsch, N. *et al.* Miniaturized iPS-Cell-Derived Cardiac Muscles for Physiologically
584       Relevant Drug Response Analyses. *Scientific Reports.* **6** 24726, (2016).
585   6   Lundy, S. D., Zhu, W. Z., Regnier, M. & Laflamme, M. A. Structural and functional
586       maturation of cardiomyocytes derived from human pluripotent stem cells. *Stem Cells and
587       Development.* **22** (14), 1991-2002, (2013).
588   7   Ma, J. *et al.* High purity human-induced pluripotent stem cell-derived cardiomyocytes:
589       electrophysiological properties of action potentials and ionic currents. *American Journal
590       of Physiology-Heart and Circulatory Physiology.* **301** (5), H2006-2017, (2011).
591   8   Sharma, A. *et al.* Use of human induced pluripotent stem cell-derived cardiomyocytes to
592       assess drug cardiotoxicity. *Nature Protocols.* 10.1038/s41596-018-0076-8, (2018).
593   9   Zhang, D. *et al.* Tissue-engineered cardiac patch for advanced functional maturation of
594       human ESC-derived cardiomyocytes. *Biomaterials.* **34** (23), 5813-5820, (2013).
595   10  Zhang, J. *et al.* Extracellular matrix promotes highly efficient cardiac differentiation of
596       human pluripotent stem cells: the matrix sandwich method. *Circulation Research.* **111** (9),
597       1125-1136, (2012).
598   11  Burridge, P. W., Holmstrom, A. & Wu, J. C. Chemically Defined Culture and Cardiomyocyte
599       Differentiation of Human Pluripotent Stem Cells. *Current Protocols in Human Genetics.* **87**
600       21 23 21-15, (2015).
601   12  Burridge, P. W. *et al.* Chemically defined generation of human cardiomyocytes. *Nature
602       Methods.* **11** (8), 855-860, (2014).
603   13  Burridge, P. W. & Zambidis, E. T. Highly efficient directed differentiation of human
604       induced pluripotent stem cells into cardiomyocytes. *Methods in Molecular Biology.* **997**
605       149-161, (2013).
606   14  Laflamme, M. A. *et al.* Cardiomyocytes derived from human embryonic stem cells in pro-
607       survival factors enhance function of infarcted rat hearts. *Nature Biotechnology.* **25** (9),
608       1015-1024, (2007).
609   15  Sharma, A. *et al.* Derivation of highly purified cardiomyocytes from human induced
610       pluripotent stem cells using small molecule-modulated differentiation and subsequent
611       glucose starvation. *Journal of Visualized Experiments.* 10.3791/52628 (97), (2015).
612   16  Bhattacharya, S. *et al.* High efficiency differentiation of human pluripotent stem cells to
613       cardiomyocytes and characterization by flow cytometry. *Journal of Visualized
614       Experiments.* 10.3791/52010 (91), 52010, (2014).
615   17  Zhang, J. *et al.* Functional cardiomyocytes derived from human induced pluripotent stem
616       cells. *Circulation Research.* **104** (4), e30-41, (2009).

617   18   Jans, D. *et al.* Action potential-based MEA platform for in vitro screening of drug-induced
618        cardiotoxicity using human iPSCs and rat neonatal myocytes. *Journal of Pharmacological*
619        *and Toxicological Methods.* **87** 48-52, (2017).
620   19   Strauss, D. G. & Blinova, K. Clinical Trials in a Dish. *Trends in Pharmacological Science.* **38**
621        (1), 4-7, (2017).
622   20   Tertoolen, L. G. J., Braam, S. R., van Meer, B. J., Passier, R. & Mummery, C. L. Interpretation
623        of field potentials measured on a multi electrode array in pharmacological toxicity
624        screening on primary and human pluripotent stem cell-derived cardiomyocytes.
625        *Biochemical and Biophysical Research Communications.* **497** (4), 1135-1141, (2018).
626   21   Braeken, D. *et al.* Open-cell recording of action potentials using active electrode arrays.
627        *Lab Chip.* **12** (21), 4397-4402, (2012).
628   22   Otsuji, T. G. *et al.* Progressive maturation in contracting cardiomyocytes derived from
629        human embryonic stem cells: Qualitative effects on electrophysiological responses to
630        drugs. *Stem Cell Research.* **4** (3), 201-213, (2010).
631   23   Shinozawa, T., Imahashi, K., Sawada, H., Furukawa, H. & Takami, K. Determination of
632        appropriate stage of human-induced pluripotent stem cell-derived cardiomyocytes for
633        drug screening and pharmacological evaluation in vitro. *Journal of Biomolecular*
634        *Screening.* **17** (9), 1192-1203, (2012).
635   24   Raphel, F. *et al.* Identification of Ion Currents Components Generating Field Potential
636        Recorded in MEA From hiPSC-CM. *IEEE Transactions on Biomedical Engineering.* **65** (6),
637        1311-1319, (2018).
638   25   Hai, A. & Spira, M. E. On-chip electroporation, membrane repair dynamics and transient
639        in-cell recordings by arrays of gold mushroom-shaped microelectrodes. *Lab Chip.* **12** (16),
640        2865-2873, (2012).
641   26   Xie, C., Lin, Z., Hanson, L., Cui, Y. & Cui, B. Intracellular recording of action potentials by
642        nanopillar electroporation. *Nature Nanotechnology.* **7** (3), 185-190, (2012).
643   27   Cohen, A., Shappir, J., Yitzchaik, S. & Spira, M. E. Reversible transition of extracellular field
644        potential recordings to intracellular recordings of action potentials generated by neurons
645        grown on transistors. *Biosensors and Bioelectronics.* **23** (6), 811-819, (2008).
646   28   Ojovan, S. M. *et al.* A feasibility study of multi-site,intracellular recordings from
647        mammalian neurons by extracellular gold mushroom-shaped microelectrodes. *Scientific*
648        *Reports.* **5** 14100, (2015).
649   29   Shmoel, N. *et al.* Multisite electrophysiological recordings by self-assembled loose-patch-
650        like junctions between cultured hippocampal neurons and mushroom-shaped
651        microelectrodes. *Scientific Reports.* **6** 27110, (2016).
652   30   Lin, Z. C., Xie, C., Osakada, Y., Cui, Y. & Cui, B. Iridium oxide nanotube electrodes for
653        sensitive and prolonged intracellular measurement of action potentials. *Nature*
654        *Communications.* **5** 3206, (2014).
655   31   Stett, A., Burkhardt, C., Weber, U., van Stiphout, P. & Knott, T. CYTOCENTERING: a novel
656        technique enabling automated cell-by-cell patch clamping with the CYTOPATCH chip.
657        *Receptors Channels.* **9** (1), 59-66, (2003).
658   32   Kanda, Y., Yamazaki, D., Osada, T., Yoshinaga, T. & Sawada, K. Development of
659        torsadogenic risk assessment using human induced pluripotent stem cell-derived
660        cardiomyocytes: Japan iPS Cardiac Safety Assessment (JiCSA) update. *Journal of*

*Pharmacological Sciences.* **138** (4), 233-239, (2018).

33      Yang, X. & Papoian, T. Moving beyond the comprehensive in vitro proarrhythmia assay: Use of human-induced pluripotent stem cell-derived cardiomyocytes to assess contractile effects associated with drug-induced structural cardiotoxicity. *Journal of Applied Toxicology.* **38** (9), 1166-1176, (2018).

34      Sala, L., Bellin, M. & Mummery, C. L. Integrating cardiomyocytes from human pluripotent stem cells in safety pharmacology: has the time come? *British Journal of Pharmacology.* **174** (21), 3749-3765, (2017).

35      Zlochiver, V., Edwards, S. & Joshi-Mukherjee, R. Longitudinal Cardiotoxic Effect of Doxorubicin in a Multicellular Cardiac Model. *Biophysical Journal.* **116** (3), 100a-101a, (2019).

36      Del Alamo, J. C. *et al.* High throuput physiological screening of iPSC-derived cardiomyocytes for drug development. *Biochimica et Biophysica Acta.* **1863** (7 Pt B), 1717-1727, (2016).

37      Clements, M. Multielectrode Array (MEA) Assay for Profiling Electrophysiological Drug Effects in Human Stem Cell-Derived Cardiomyocytes. *Current Protocols in Toxicology.* **68** 22 24 21-22 24 32, (2016).

38      Navarrete, E. G. *et al.* Screening drug-induced arrhythmia [corrected] using human induced pluripotent stem cell-derived cardiomyocytes and low-impedance microelectrode arrays. *Circulation.* **128** (11 Suppl 1), S3-13, (2013).

39      Harris, K. *et al.* Comparison of electrophysiological data from human-induced pluripotent stem cell-derived cardiomyocytes to functional preclinical safety assays. *Toxicological Sciences.* **134** (2), 412-426, (2013).

40      Zlochiver, V., Edwards, S. L. & Joshi-Mukherjee, R. Longitudinal Cardiotoxic Effect of Doxorubicin in a Multicellular Cardiac Model. *Biophysical Journal.* **116** (3), 100a-101a, (2019).

41      Waas, M. *et al.* Are These Cardiomyocytes? Protocol Development Reveals Impact of Sample Preparation on the Accuracy of Identifying Cardiomyocytes by Flow Cytometry. *Stem Cell Reports.* 10.1016/j.stemcr.2018.12.016, (2019).

42      Gorospe, G. *et al.* Automated grouping of action potentials of human embryonic stem cell-derived cardiomyocytes. *IEEE Transactions on Biomedical Engineering.* **61** (9), 2389-2395, (2014).

43      Zhu, W., Varga, Z. & Silva, J. R. Molecular motions that shape the cardiac action potential: Insights from voltage clamp fluorometry. *Progress in Biophysics & Molecular Biology.* **120** (1-3), 3-17, (2016).

Figure 1

## A



## B

Figure 2

## A



electrode arrays

reference electrodes

## B
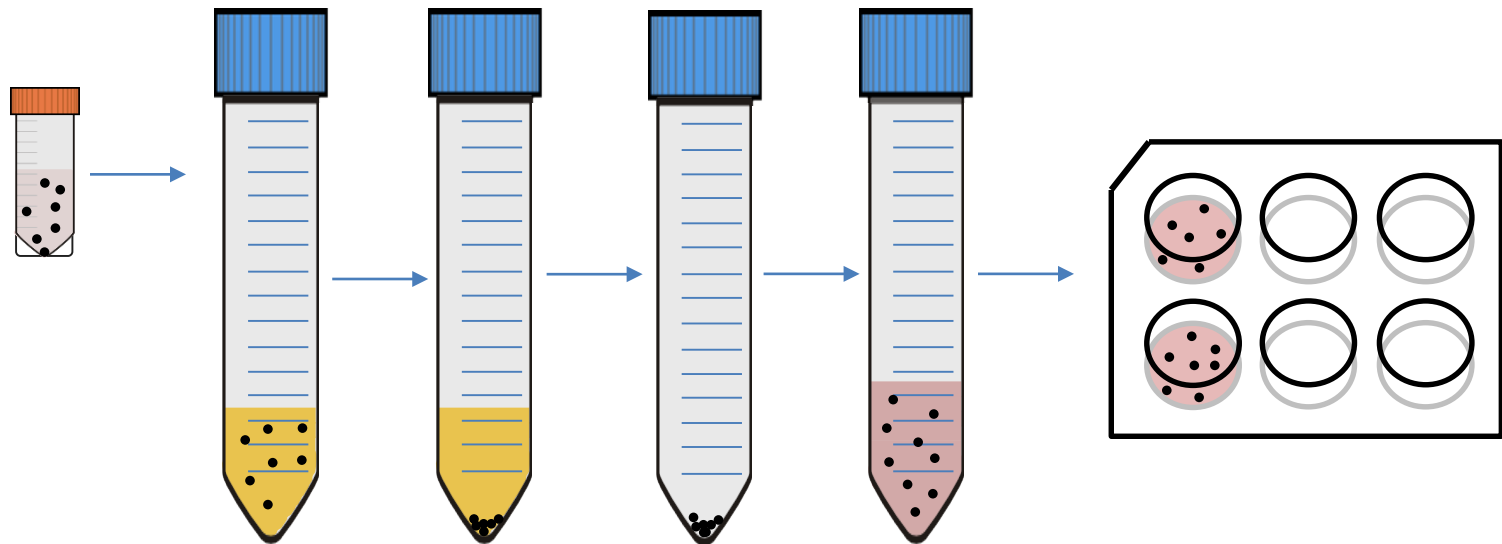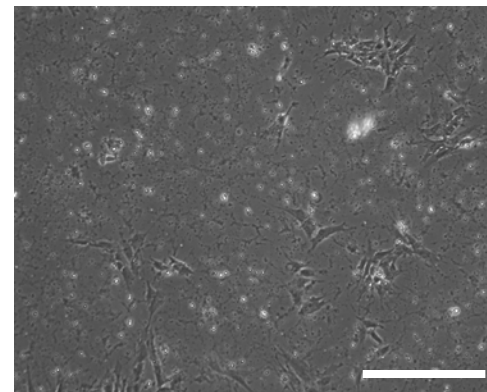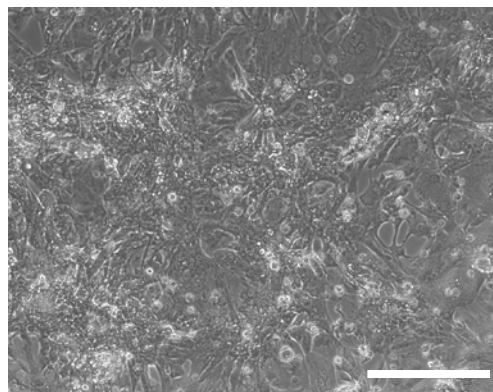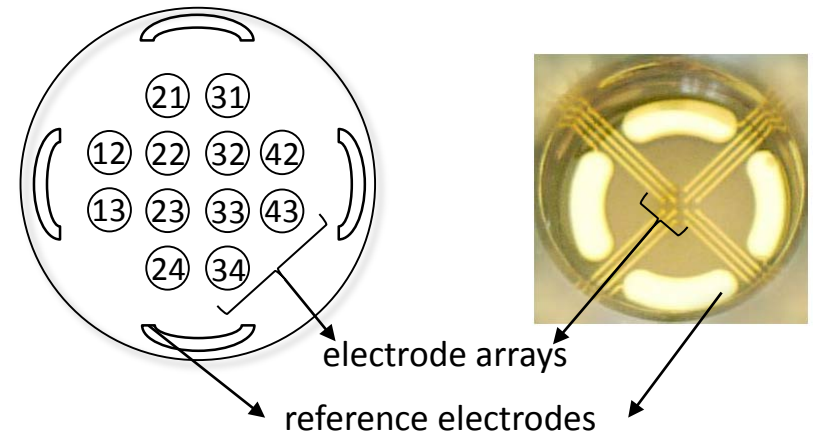


| Wash with **sterile ddH$_2$O** and record baseline | Sterilize under **UV light** | Hydrophilic **FBS** treatment | Wash with **sterile ddH$_2$O** twice | Dry overnight |

Figure 3

A



B



C

Figure 4

Click here to access/download;Figure;Figure 4.pdf ⬇
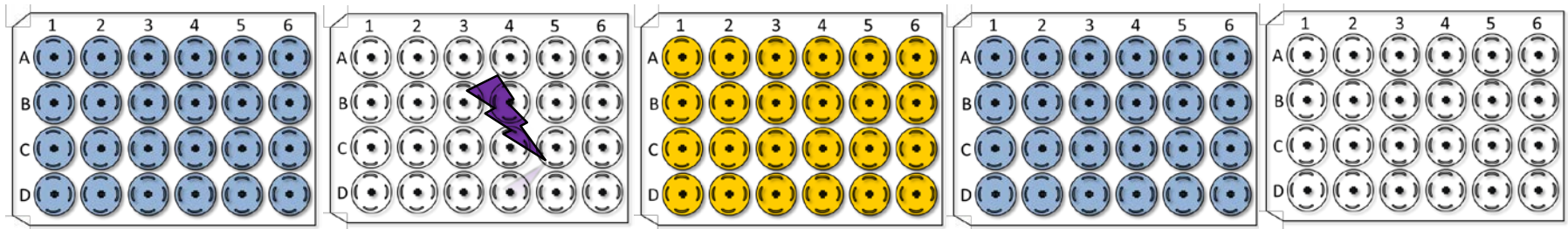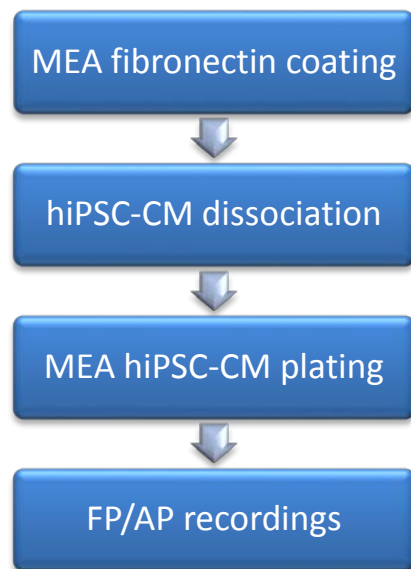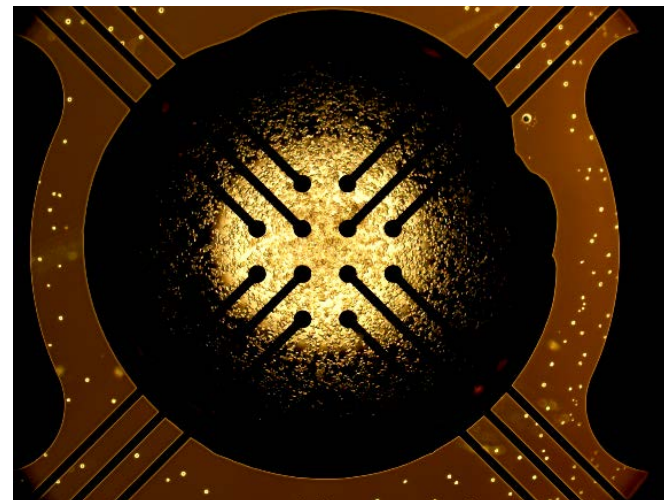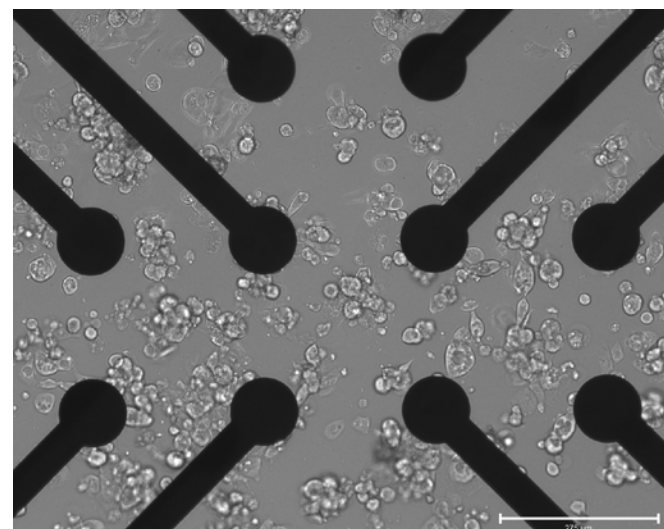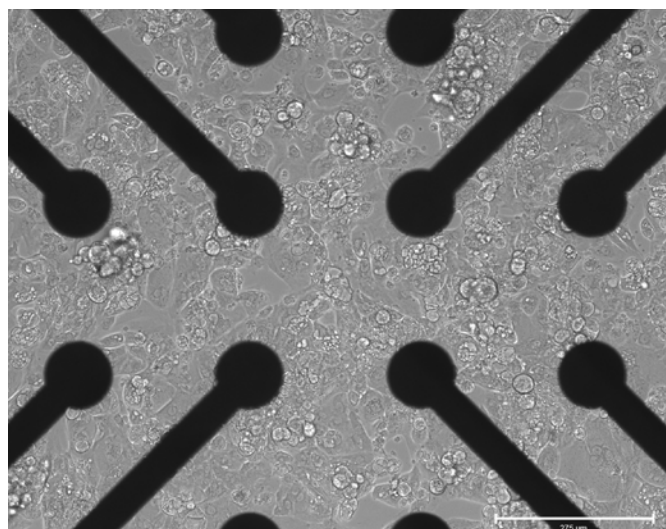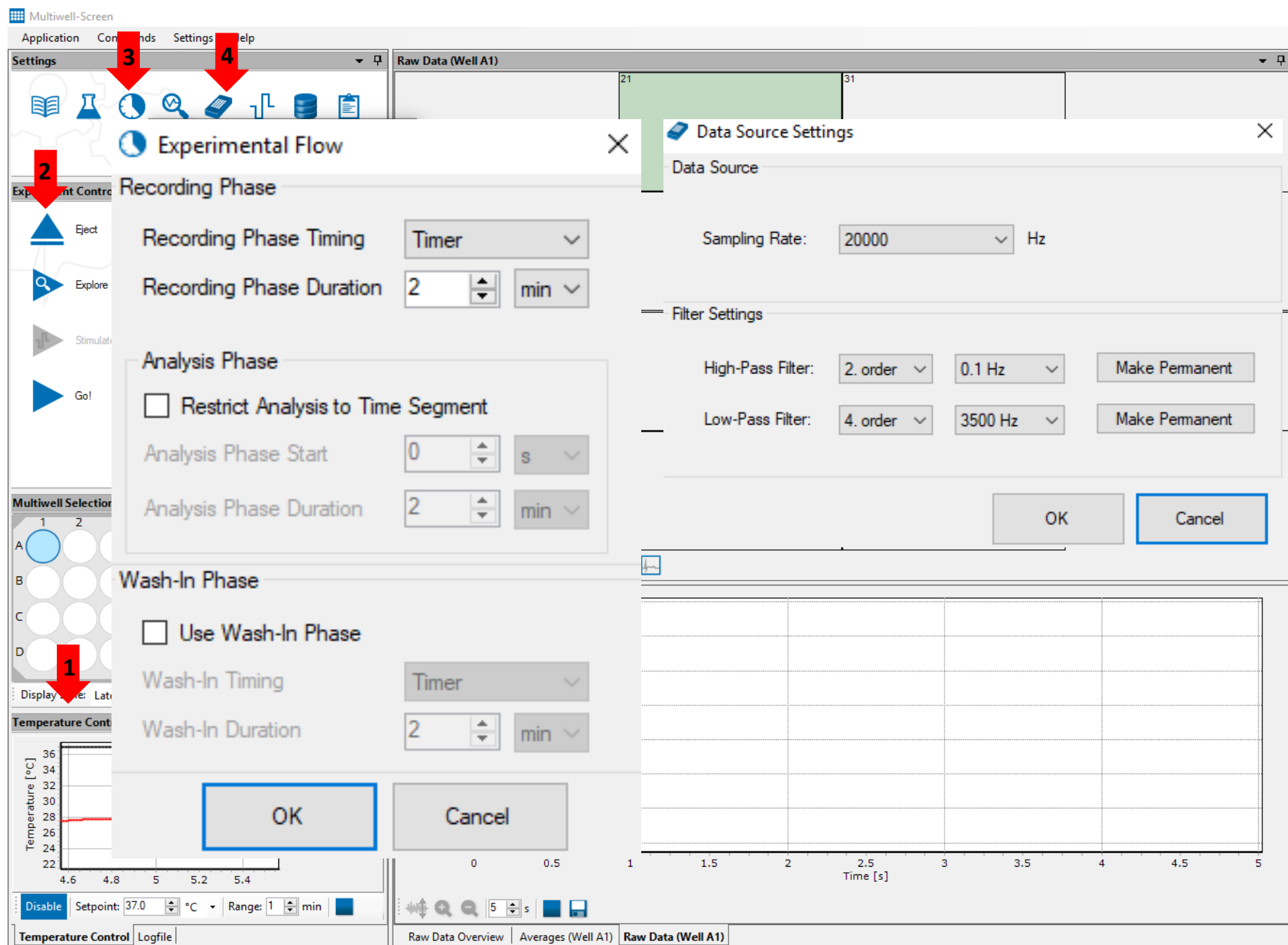
Figure 5

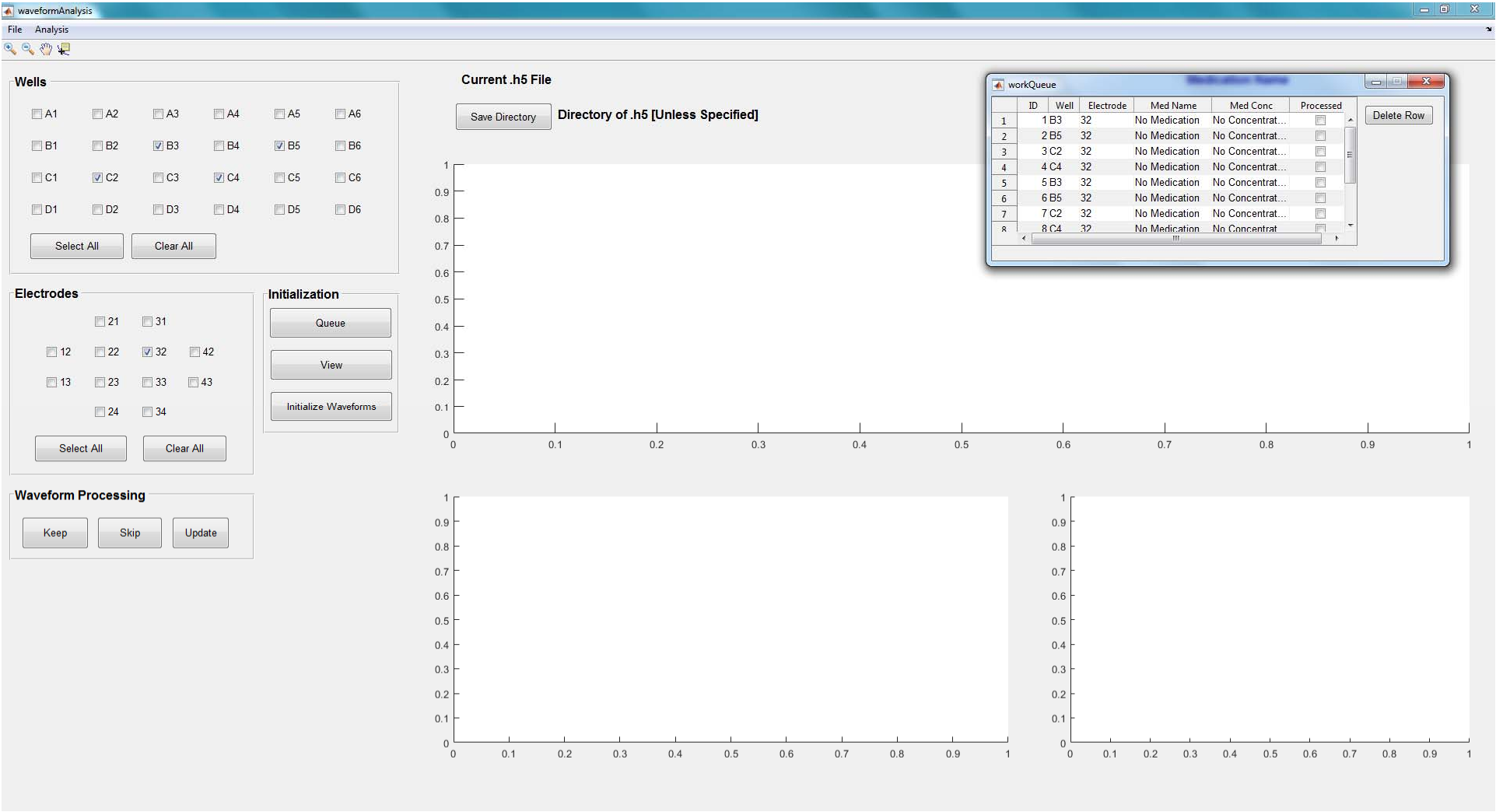Click here to access/download;Figure;Figure 5.pdf ⬇
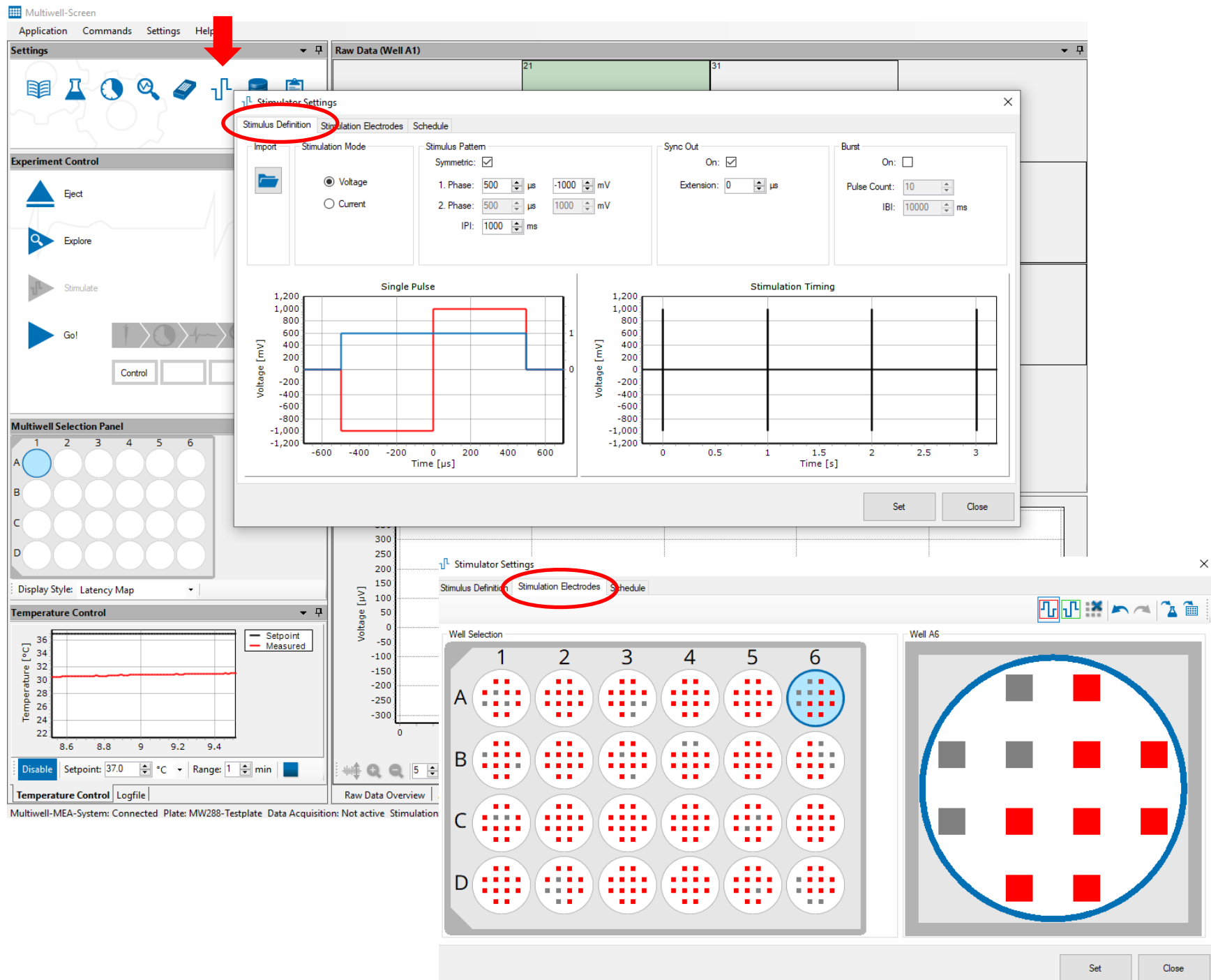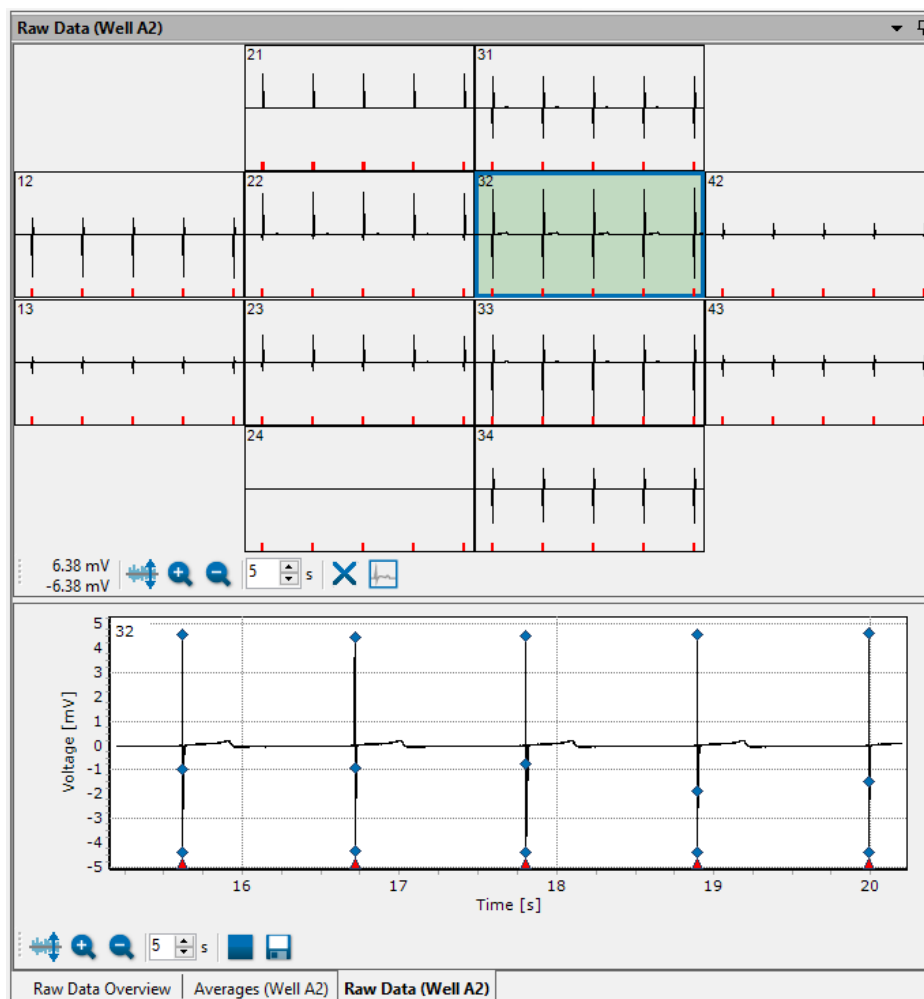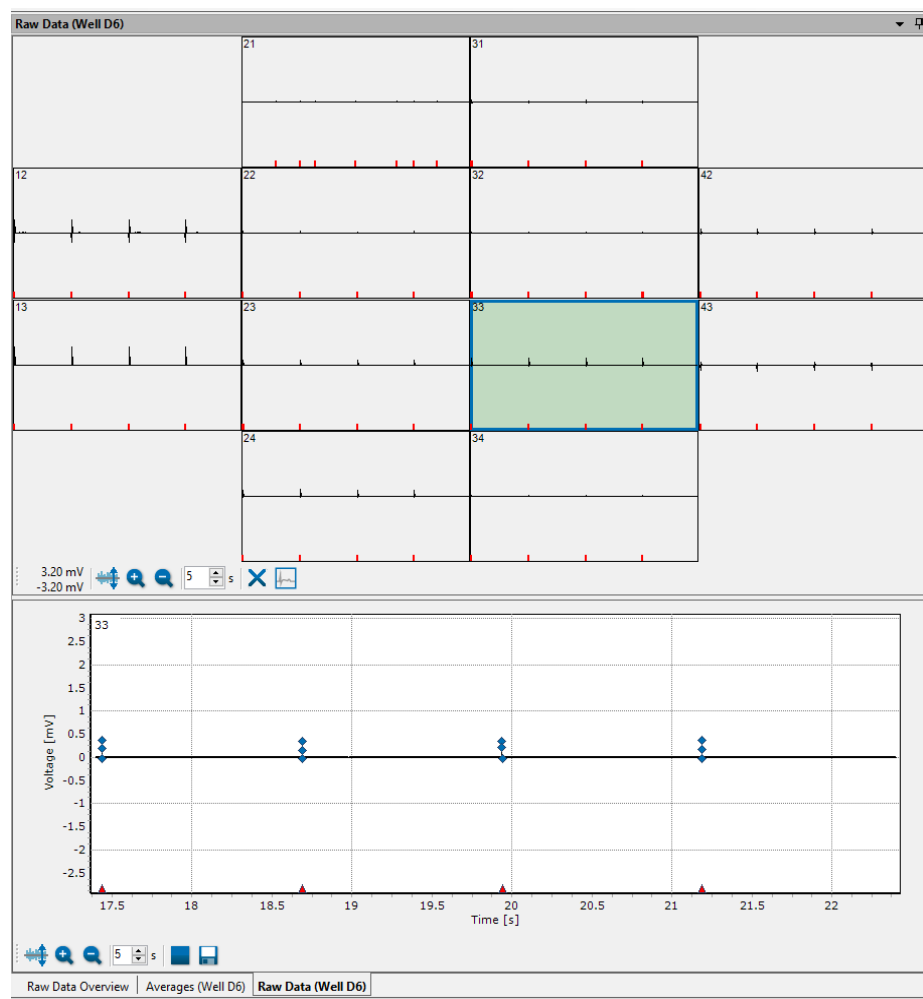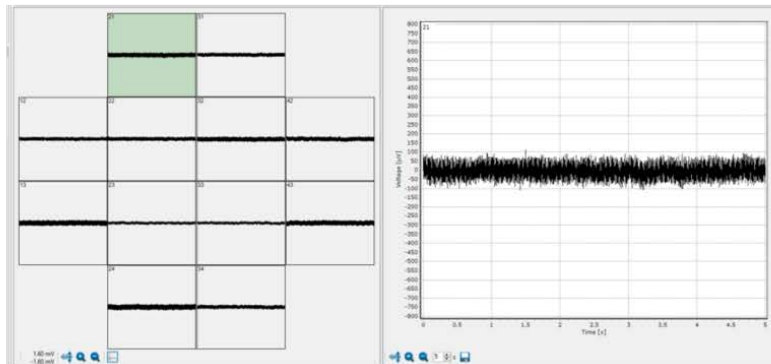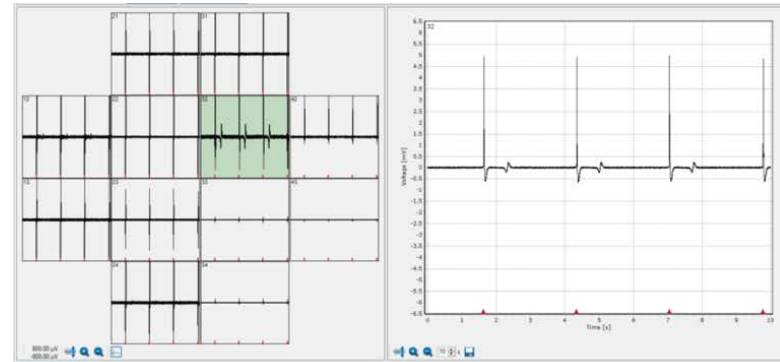
Figure 6

Click here to access/download;Figure;Figure 6.pdf ⬇

Figure 7

**A**



**B**



**C**

Figure 8

Figure 9
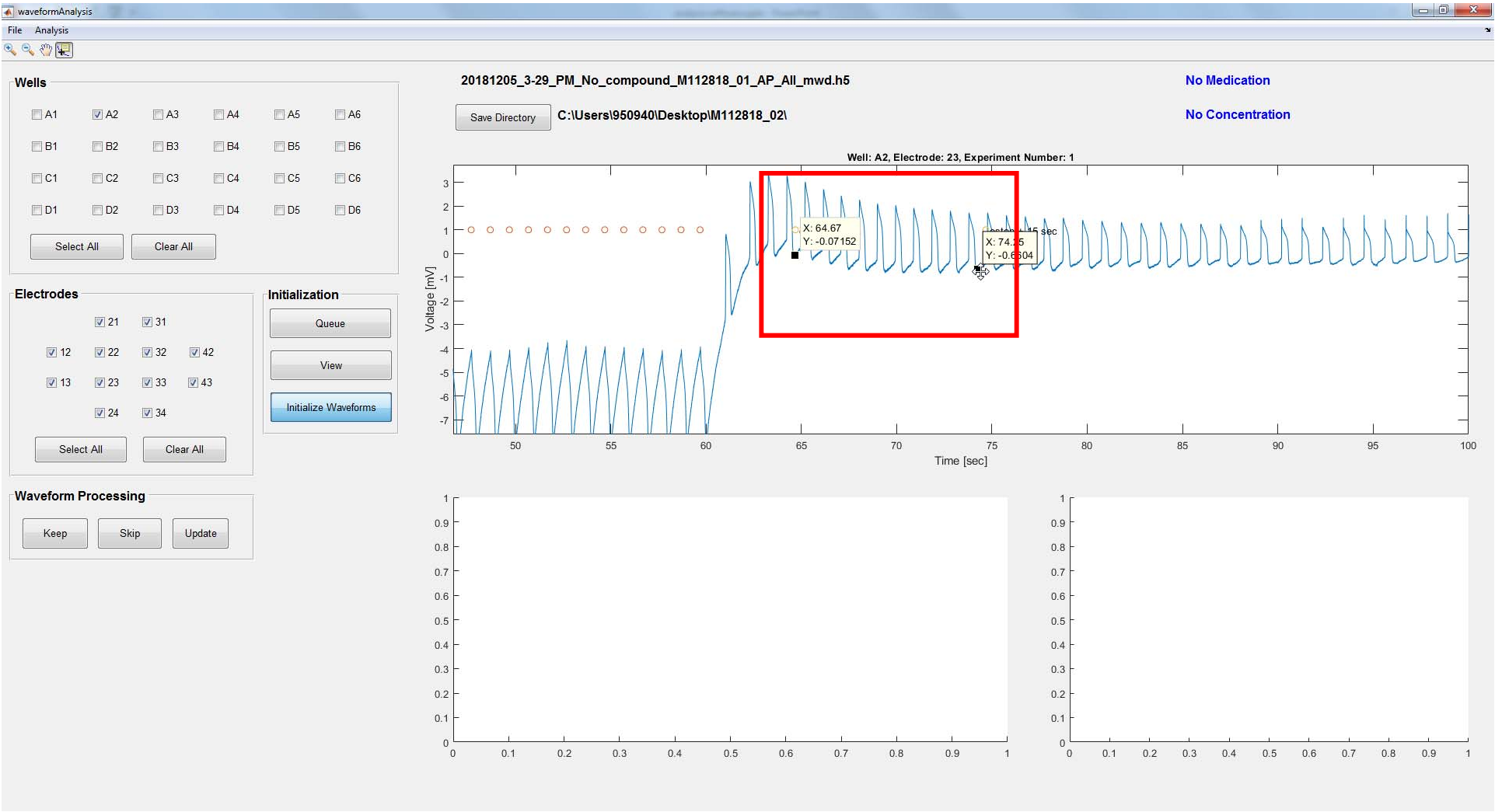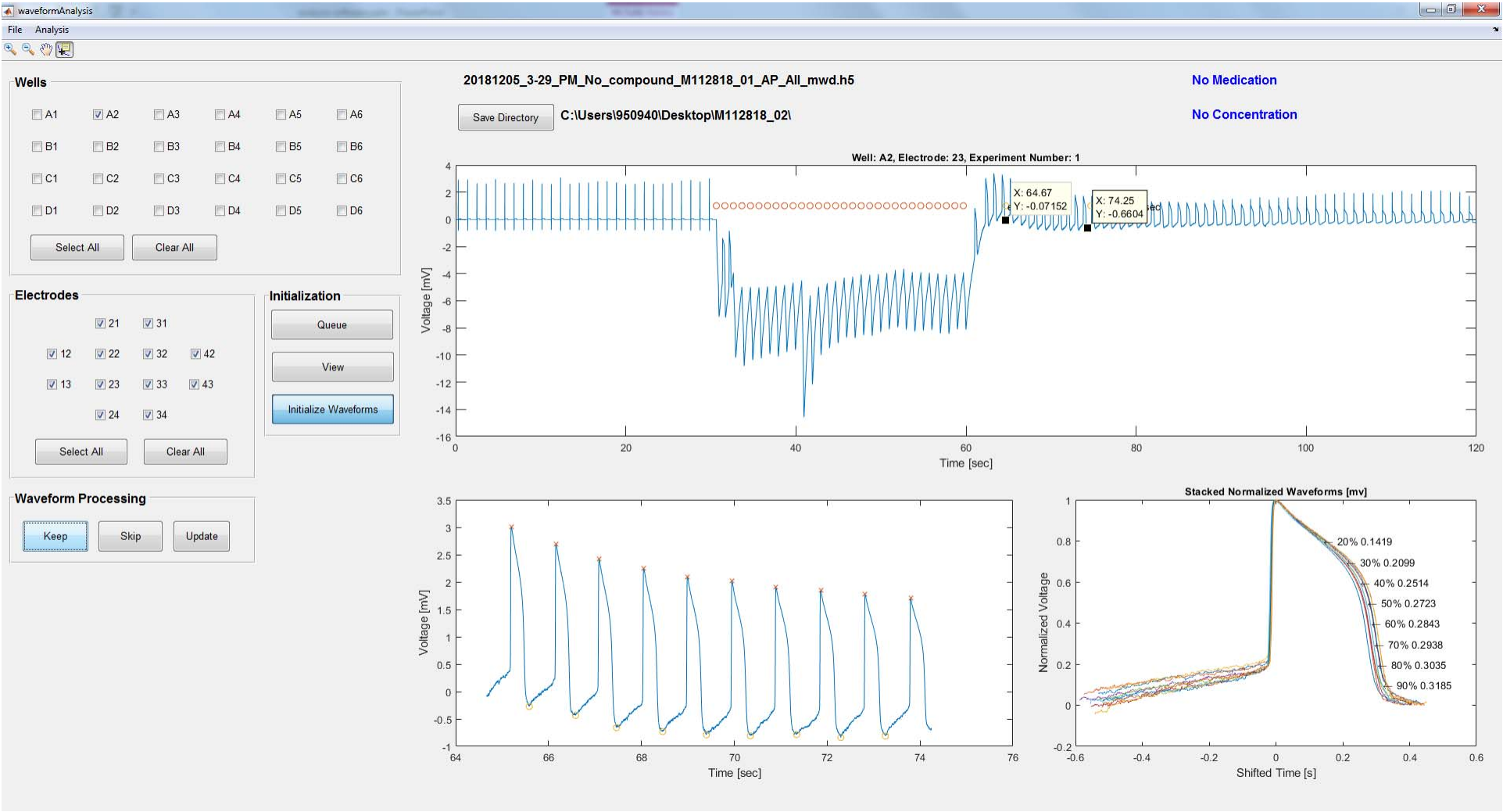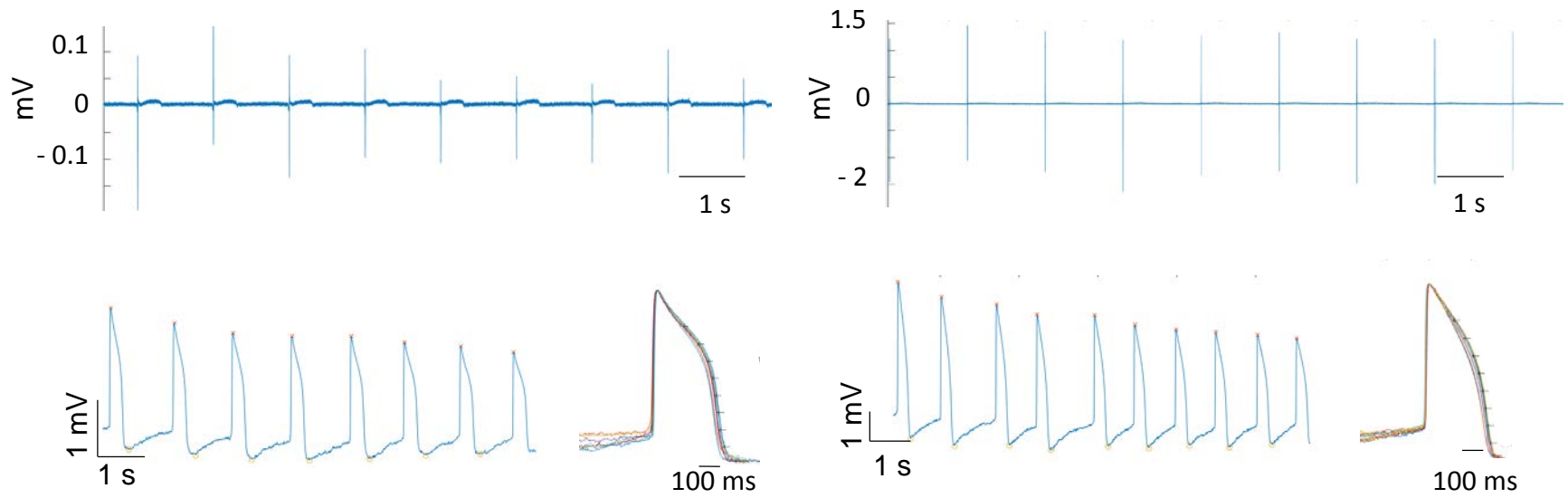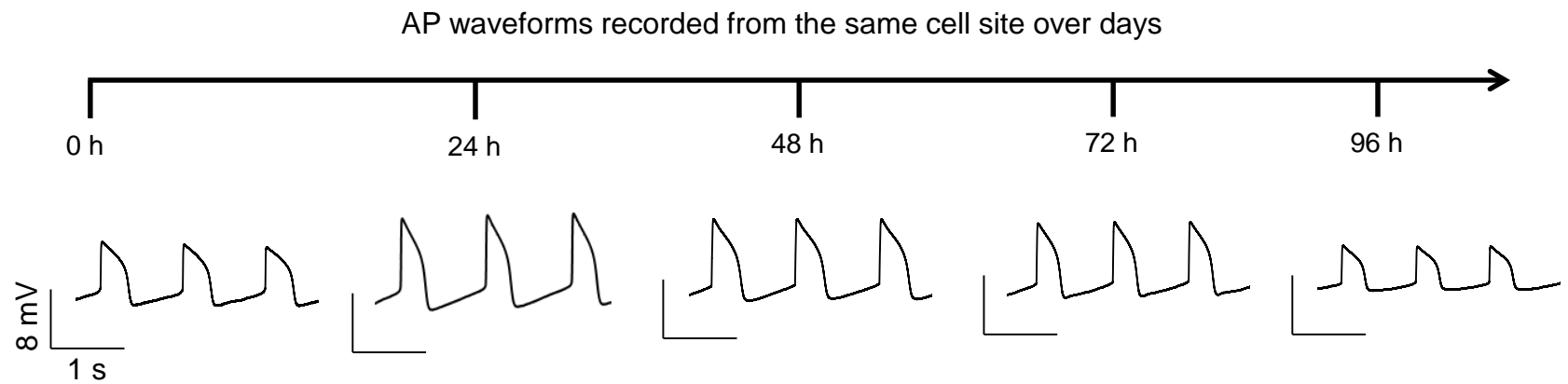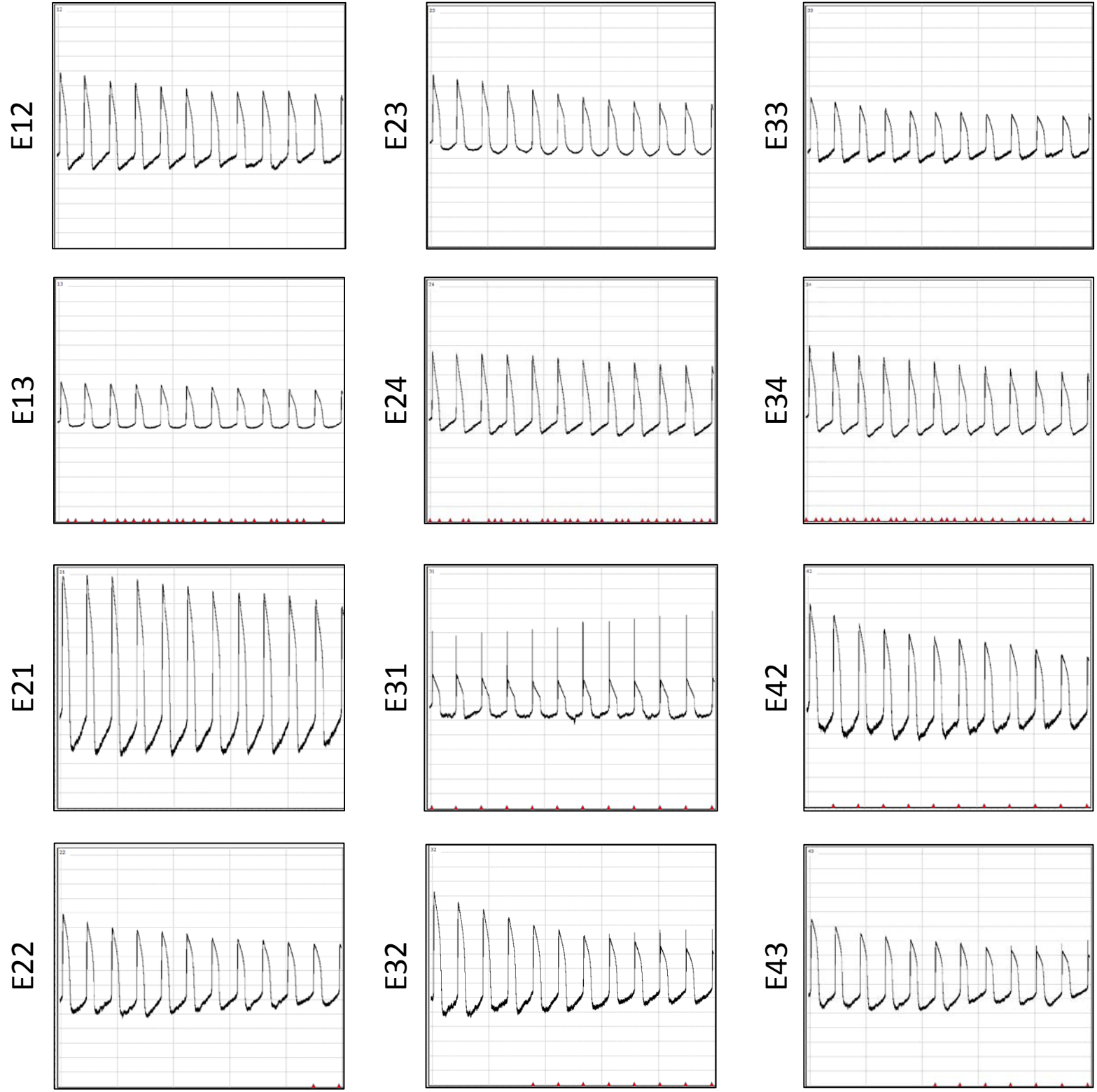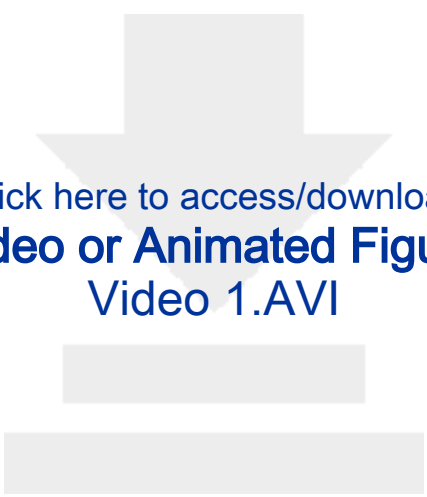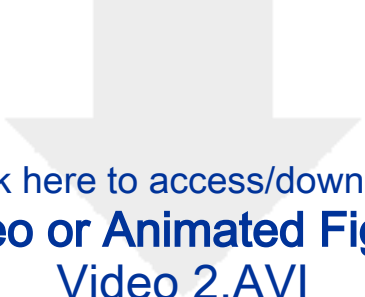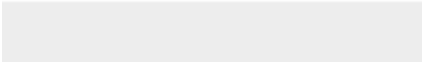
Figure 10

Figure 11

AP waveforms recorded from the same cell site over days

Figure 12

Figure 12

Figure 13
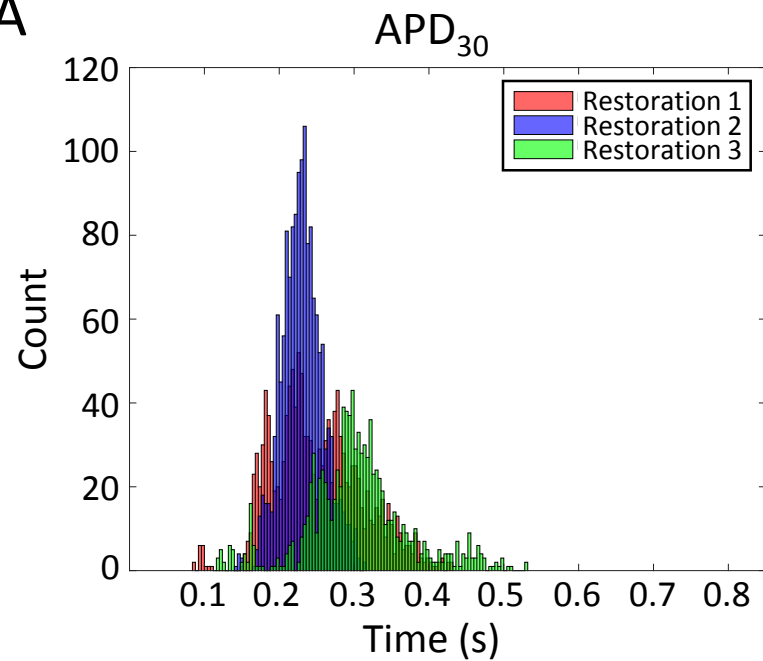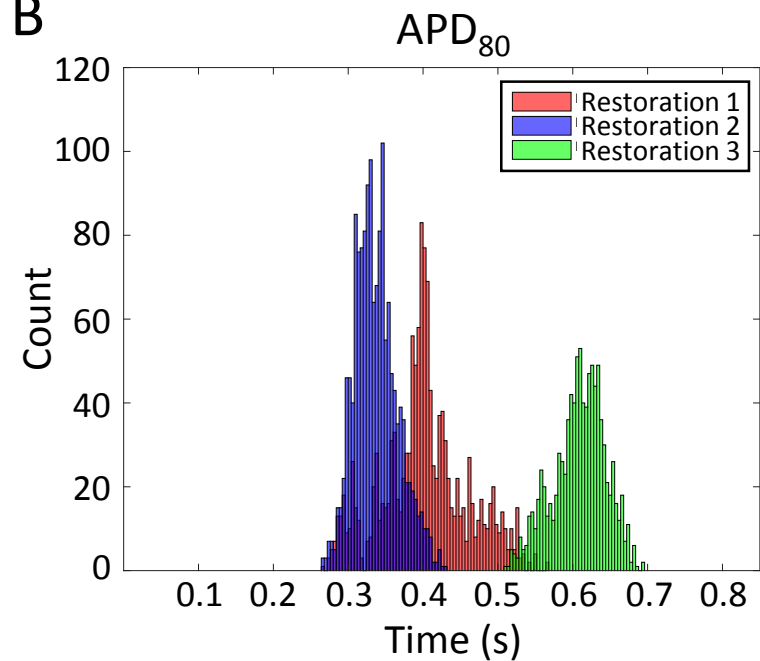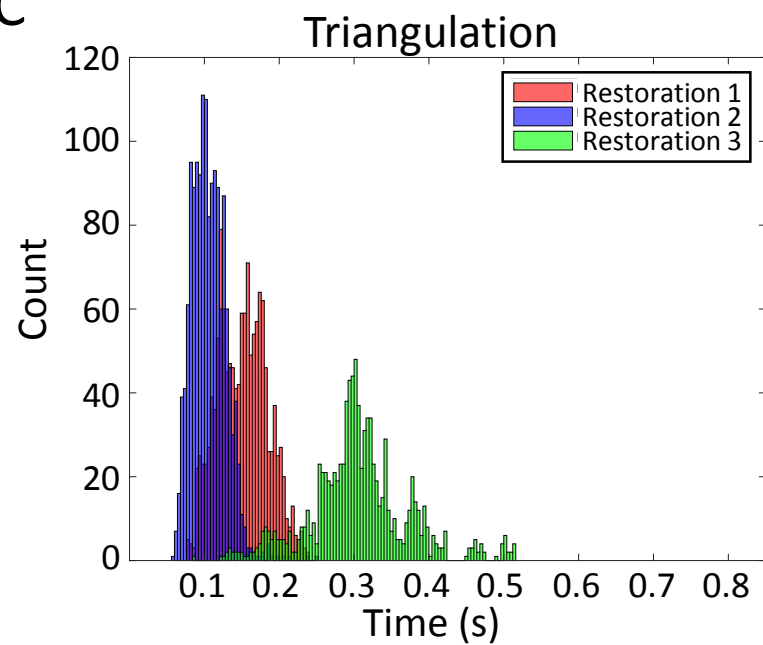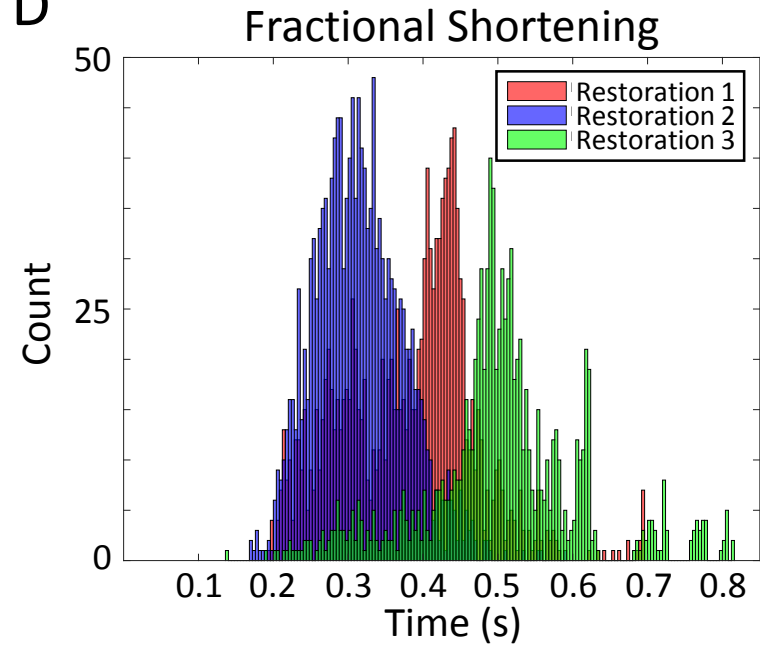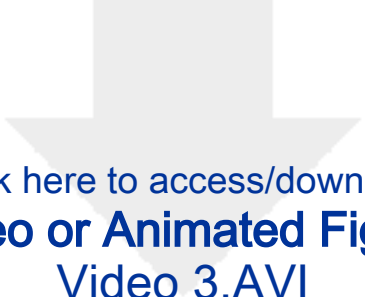
Figure 13

Video 1

Click here to access/download
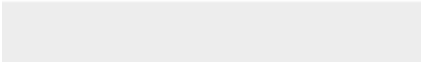**Video or Animated Figure**
Video 1.AVI

Click here to access/download
**Video or Animated Figure**
Video 2.AVI

Click here to access/download
**Video or Animated Figure**
Video 3.AVI

| Name of Reagent/ Equipment | Company | Catalog Number | Comments |
|---|---|---|---|
| Accutase | Sigma Aldrich | A6964-100ML | cell dissociation solution |
| Acquisition software | Multichannel Systems | Multiwell-Screen v 1.9.2.0 | |
| B27 Supplement | ThermoFisher | 17504-044 | CM media supplement |
| Converter software | Multichannel Systems | MultiChannel DataManager | |
| DMEM/F12 | ThermoFisher | 11330-032 | |
| D-PBS | ThermoFisher | 14190-250 | |
| FBS | Fisher Scientific | SH3007103HI | |
| Fibronectin | Sigma Aldrich | F1141-5MG | |
| Geltrex | ThermoFisher | A1413202 | coating substrate |
| Interface board | Multichannel Systems | MCS-IFB 3.0 Multiboot Interface Board | |
| Multiwell MEA Plate | Multichannel Systems | 24W300/30G-288 | |
| RPMI 1640 | ThermoFisher | 11875-093 | CM base medium |
| Terg-a-zyme | Sigma Aldrich | Z273287-1EA | enzymatic detergent |
| Transfer pipettes, individually wrapped | Fisher Scientific | 1371148 | |
| Trypan Blue | Sigma Aldrich | T8154-100ML | |
| Ultrapure sterile water | ThermoFisher | 10977-023 | |
| 6-well tissue-culture treated plates | Fisher Scientific | 08-772-1B | |

This piece of the submission is being sent via mail.

Aurora Research Institute™

*Aurora Sinai Medical Center*
*960 N. 12th Street*
*Milwaukee, WI 53233*
*Phone: 414-219-7502*
*Rosy.joshi-mukherjee@aurora.org*

April 19th, 2019

Bing Wu, Ph.D.
Review Editor
Journal of Visualized Experiments (JoVE)

Re: JoVE59906_R1 "Human iPSC-Derived Cardiomyocyte Networks on Multiwell Micro-Electrode Arrays for Recurrent Label-free Action Potential Recordings,"

Dear Dr. Wu,

Sincerest thanks for your prompt response. We are pleased to know that we addressed all peer reviewers' comments and have modified the manuscript to address the remaining editorial comments. We used 'track changes' for easy reference.

Thank you for your consideration of our work. Please address all correspondences concerning this manuscript to me via email (rosy.joshi-mukherjee@aurora.org).

Sincerely,

Rosy Joshi-Mukherjee, PhD

Research Scientist